Catalysis Science & Technology

PAPER

View Article Online
View Journal



Cite this: DOI: 10.1039/c5cy01409c

# Poisoning of vanadia based SCR catalysts by potassium: influence of catalyst composition and potassium mobility

Brian K. Olsen,[a] Frauke Kügler,[ab] Francesco Castellino[c] and Anker D. Jensen*[a]

Received 26th August 2015,
Accepted 13th November 2015

DOI: 10.1039/c5cy01409c

www.rsc.org/catalysis

The deactivation of $V_2O_5$–$(WO_3)/TiO_2$ catalysts for selective catalytic reduction (SCR) of $NO_x$ upon exposure to aerosols of KCl or $K_2SO_4$, at different temperatures, has been studied. All samples exposed for more than 240 hours lost a substantial fraction of their initial activity although lower exposure temperatures slow down the deactivation. $K_2SO_4$ causes a lower rate of deactivation compared to KCl. This may be related to a faster transfer of potassium from the solid KCl matrix to the catalyst, however, it cannot be ruled out to also be caused by a significantly larger particle size of the $K_2SO_4$ aerosol (mass based distribution mode: 1.3 μm) compared to that of the KCl aerosol (mass based distribution mode: 0.12 μm). The relative activities of exposed catalysts indicate that promotion with $WO_3$ accelerates the deactivation, likely due to the enhanced Brønsted acidity which appears to promote the transport of potassium. Using a newly developed experimental protocol consisting of two-layer pellets of SCR catalysts, where one side is impregnated with KCl or $K_2SO_4$, the potassium transport in such systems, which is assumed to take place through reaction and diffusion over acid sites, was investigated. SEM-WDS measurements on pellets heat treated at 350 °C show that potassium bound in KCl readily leaves its counter ion and thus moves faster into the catalyst compared to potassium from $K_2SO_4$, which is in agreement with results from the aerosol exposures.

## 1. Introduction

Selective catalytic reduction (SCR) of nitrogen oxides ($NO_x$) with ammonia ($NH_3$) is a well established method for controlling the $NO_x$ emissions from stationary sources such as coal fired heat and power plants.[1,2] The most widely used catalysts for such applications consist of vanadia ($V_2O_5$) supported on titania ($TiO_2$), promoted with either tungsten oxide ($WO_3$) or molybdenum oxide ($MoO_3$), in the shape of honeycomb monoliths.[2,3] Topsøe and co-workers[4–6] proposed a mechanism for the SCR reaction over $V_2O_5$ based catalysts consisting of two catalytic cycles, involving Brønsted acid sites ($V^{5+}$–OH) and redox sites ($V^{5+}$=O). In the presence of hydrogen chloride (HCl), $V_2O_5$–$WO_3/TiO_2$ SCR catalysts are furthermore active in the oxidation of elemental mercury ($Hg^0$), another emission from coal fired power plants, to the more soluble (hence easily removable) $Hg^{2+}$.[7,8]

In a time with great focus on decreasing the release of carbon dioxide ($CO_2$) to the atmosphere, firing (or co-firing) of biomass (straw, wood chips *etc.*) is being applied to substitute fossil fuels in order to reduce the net $CO_2$ emissions. Unfortunately, alkali and alkaline earth metals, which can be present in biomass in high concentrations,[9] may act as poisons to the industrially applied SCR catalysts and can reduce their life-time dramatically, especially when the catalysts are used in high-dust configuration.[10] Potassium, released *e.g.* during firing of straw, may form submicron aerosols of potassium chloride (KCl) and/or potassium sulfate ($K_2SO_4$)[11,12] which can deposit on the external catalyst surface. Most likely through a surface diffusion mechanism, potassium subsequently diffuses into the catalyst wall.[13–15] It is believed that potassium, due to its alkaline nature, poisons the SCR catalyst by reacting with the acidic $V^{5+}$–OH sites.[10,14,16–22] It has furthermore been shown that the reducibility of $V^{5+}$=O species is inhibited upon alkali poisoning, which slows down the catalytic cycle.[20–25] While the effect of potassium on commercial SCR catalysts, as outlined above, is generally well understood, a more systematic study of the deactivation mechanism will provide useful information for development of new alkali resistant catalysts and/or improved means of operation. To our knowledge, there are no systematic studies of the influence of catalyst composition on the rate of potassium uptake and the associated deactivation. Furthermore, there are no systematic studies of the influence of the aerosol size distribution on the rate of deactivation. It is conceivable that the aerosol size distribution

[a] Department of Chemical and Biochemical Engineering, Technical University of Denmark, Søltofts Plads 229, 2800 Kgs. Lyngby, Denmark. E-mail: aj@kt.dtu.dk
[b] Department of Energy Process Engineering and Chemical Engineering, Technical University of Freiberg, Fuchsmühlenweg 9, 09596 Freiberg, Germany
[c] Haldor Topsøe A/S, Nymøllevej 55, 2800 Kgs. Lyngby, Denmark

may significantly influence the rate of deactivation since: 1) the rate of deposition of aerosol particles increases with decreasing size due to their higher diffusion velocity and 2) the rate of potassium uptake is likely to depend on the volume (or mass) based contact area with the catalyst material which is smaller for larger particles (contact area/particle volume $\sim 1/d_p$, with $d_p$ being the aerosol particle diameter). Finally, the influence of catalyst operating temperature on the rate of deactivation has not previously been investigated in depth.

In this work, the deactivation by potassium poisoning of $V_2O_5$–$(WO_3)/TiO_2$ based catalyst plates, of various composition, have been studied. The plates have been exposed to KCl or $K_2SO_4$ aerosols of different particle size at various temperatures in a bench-scale setup, and tested for remaining activity in a lab-scale reactor. Furthermore, the mobility of potassium in SCR catalysts have been studied by a newly conceived experimental protocol in which pellets consisting of one undoped layer and one layer of potassium impregnated SCR catalyst are heat treated in a lab-scale oven, followed by measurement of the resulting potassium profiles across the pellet width using Scanning Electron Microscopy/Wavelength Dispersive X-ray Spectroscopy (SEM-WDS). These experiments provide detailed information on the rate of potassium diffusion in SCR catalysts.

# 2. Experimental

### 2.1. Catalysts

Plate shaped catalysts supplied by Haldor Topsøe A/S were used in this study. The catalysts were based on $V_2O_5$, with approximate loadings of 1, 3 and 6 wt%, on a fiber reinforced $TiO_2$ carrier. Some plates were promoted with about 7 wt% $WO_3$. The catalysts have a tri-modal pore structure which mainly consists of meso- and macropores, with pore diameter modes of roughly 10 nm, 300 nm and 10–20 μm.[26] The Brunauer–Emmett–Teller surface area of the catalysts is around 60–80 $m^2\ g^{-1}$.[10,26] The structural properties are not expected to vary significantly between the individual catalysts, at vanadia loadings below monolayer coverage. Upon delivery, the catalyst plates had dimensions (thickness × width × height) of 1 mm × 50 mm × 148–166 mm, from which pieces with dimensions of 36 mm × 98 mm were cut from the individual plates and used for the bench-scale exposure campaigns.

### 2.2. Bench-scale aerosol exposure

The plates were exposed to aerosols of KCl or $K_2SO_4$ in a bench-scale reactor previously used for a similar study by Zheng *et al.*[14] The setup, illustrated in Fig. 1, consists of a natural gas burner, a flue gas duct perpendicular to the burner outlet, a heat exchanger section where the reactor temperature can be controlled, and the reactor itself. The reactor can house a full-length (50 cm) SCR monolith or, as was the case in this study, a set of up to nine plate-type catalysts placed in a steel cassette in the top part of the reactor. A second heat exchanger cools the flue gas further before it is led to the stack.

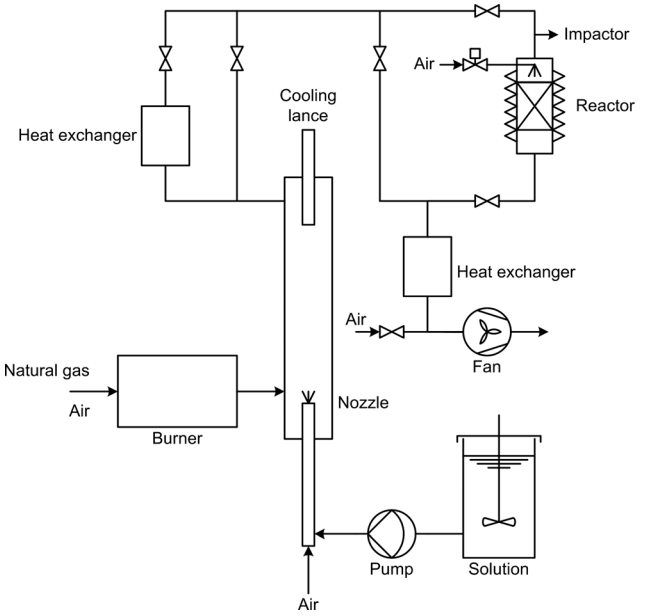


Fig. 1 Schematic drawing of the bench-scale setup for aerosol exposure of SCR catalyst plates.

A water cooled injector probe, equipped with a two-fluid nozzle, can be introduced into the flue gas duct at the end adjoining the burner outlet. At the opposite end of the duct, a bayonet heat exchanger can be inserted for further cooling. Aerosols of either KCl or $K_2SO_4$ were generated by pumping an aqueous solution of the respective salt (with a concentration of 0.1 M with respect to potassium ions) through the injector probe, at a rate of 420 mL $h^{-1}$, and injecting it into the hot flue gas by the aid of pressurized air through the two-fluid nozzle.

In addition to being heated by the flue gas, the SCR reactor was heated from the outside by an electrical heating cable and insulated by a mantle of mineral wool in order to minimize radial temperature gradients. The axial temperature gradient over the catalysts was always within 5 °C. In order to avoid build-up of particles on top of the catalyst cassette, a burst of pressurized air from a soot blower, located above the reactor, was released for approximately 1 second every 30 minutes. The total gas flow through the reactor was 35–45 $Nm^3\ h^{-1}$ corresponding to a linear gas velocity of 1.7–2.2 Nm $s^{-1}$ (0 °C, 1 atm, empty reactor). Six exposure campaigns have been conducted in this study. The campaigns differed by the injected salt solution, the SCR reactor temperature, the total exposure time and the position of the injector nozzle leading to different temperatures for the aerosol particle formation. Up to nine catalyst plates were exposed in each campaign.

### 2.3. Aerosol measurement

The mass based particle size distribution was measured by a 10-stage Berner-type low pressure impactor (LPI, Hauke Ges.

 

m.b.H. & Co.KG) with an aerodynamic diameter range of 0.03–12.7 μm. The gas was sampled above the reactor inlet through a straight cylindrical tube perpendicular to the main flow at a flow rate of 23.11 NL $min^{-1}$. In order to avoid water condensation, the sampling tube and the impactor were heated to 90 °C. The sampling time was 60 minutes. The particles were collected on aluminum foils coated with a thin film of Apiezon H vacuum grease. The grease was added by applying a thin layer of a dilute solution of the grease in toluene onto the foils. In order to remove the toluene, the foils were dried in an oven at 140 °C for several hours.

### 2.4. Activity measurement

The catalytic activities of the exposed samples, as well as unexposed counterparts, were measured in the laboratory at temperatures between 250 and 400 °C. The samples were crushed to a powder, diluted with sand and loaded into a quartz reactor between two layers of quartz wool. A typical reactor loading contained 50–100 mg catalyst. A total flow of about 2800 NmL $min^{-1}$ was used during the measurements and the gas was composed of 500 ppmv NO, 600 ppmv $NH_3$, 5 vol% $O_2$, about 1.4 vol% $H_2O$ and balance $N_2$. The $H_2O$ content was obtained by saturating a stream of $N_2$ at room temperature by passing it through a bubble flask with water. The dry NO concentration at the reactor outlet was measured by a Rosemount NGA 2000 analyzer.

The NO reduction in the SCR reaction can be described by an Eley–Rideal rate expression where $NH_3$ adsorbs on the catalyst surface while NO reacts from the gas phase with the adsorbed species.[27–29] This mechanism leads to the following rate expression:

$$-r_{NO}\left[\frac{\text{kmol}}{\text{kg s}}\right] = k_r C_{NO}\frac{K_{NH3}C_{NH3}}{1+K_{NH3}C_{NH3}} \quad (1)$$

Here $k_r$ ($m^3$ $kg^{-1}$ $s^{-1}$) is the intrinsic rate constant, $C_i$ (kmol $m^{-3}$) is the concentration of component $i$ in the gas phase, while $K_{NH3}$ ($m^3$ $kmol^{-1}$) is the $NH_3$ adsorption equilibrium constant. When $NH_3$ is in excess, eqn (1) can be reduced to a pseudo first order expression with respect to NO:

$$-r_{NO} = k' C_{NO} \quad (2)$$

For a first order reaction with plug flow in a packed-bed reactor, the pseudo first order rate constant, $k'$, can be calculated from eqn (3):

$$k'\left[\frac{\text{m}^3}{\text{kg s}}\right] = -\frac{F_{gas}}{m_{cat}}\ln\left(1-X_{NO}\right) \quad (3)$$

Where $F_{gas}$ ($m^3$ $s^{-1}$) is the gas flow rate at reactor conditions, $m_{cat}$ (kg) is the catalyst mass and $X_{NO}$ is the NO conversion. In the following the rate constant/catalytic activity of an exposed sample will be reported relative to that of the same catalyst in its fresh state, $k'_0$.

### 2.5. Ammonia chemisorption

In order to have a measure of the amount of active acid sites as a function of catalyst composition, $NH_3$ chemisorption measurements, similar to those carried out by Zheng *et al.*[10] have been performed on fresh catalysts. Pieces of 16 mm × 16 mm (corresponding to 0.62–0.68 g) were cut from the individual catalyst plates and placed in a quartz reactor which was heated to 250 °C. A gas mixture of 600 ppmv $NH_3$, 5 vol% $O_2$ and about 1.5 vol% $H_2O$ in $N_2$ was passed over the catalyst for 30 minutes, which was found sufficient in order to saturate the active sites with $NH_3$. The $NH_3$ flow was then shut off and about 500 ppmv NO was added to the reactor shortly after. The amount $NH_3$ adsorbed on active sites could then directly be correlated to the amount of NO reduced by $NH_3$, assuming that the reaction followed the standard SCR reaction:

$$4NO + 4NH_3 + O_2 \rightarrow 4N_2 + 6H_2O \quad (4)$$

A temperature of 250 °C was chosen in order to reduce the desorption of $NH_3$ as the flow was shut off, while still retaining some SCR activity.

### 2.6. Two-layer pellet experiments

To investigate the transport of potassium in the catalyst under more controlled conditions, pellets consisting of two layers of crushed plate catalyst in close contact were produced. One layer was made from a fresh $V_2O_5$–($WO_3$)/$TiO_2$ catalyst, while the other layer was made of the same catalyst doped with either KCl or $K_2SO_4$ to a potassium level of 0.8–1.6 wt%. The potassium doping was achieved by wet impregnation of whole catalyst plates which were subsequently dried at 80 °C, crushed, and (in some cases) calcined at 400 °C overnight. Initially, one side of the pellet was made by partial compression of the powder in a pellet die. The powder of the other side was then added to the die and a final compression pressure of 60 bar was applied for 1 minute. Each pellet consisted of about 600 mg of pulverized catalyst (300 mg in each layer) and had a diameter of 13 mm and a thickness of 2.3 mm. A principle sketch of a two-layer pellet is shown in Fig. 2. A pellet composed of a layer of pure KCl salt, crushed and sieved to a fraction below 250 μm, and a layer of fresh 3% $V_2O_5$–7% $WO_3$/$TiO_2$ catalyst powder was also produced. The pellets were exposed at 350 °C for up to 7 days in a horizontal lab-scale reactor, illustrated in Fig. 3. During the

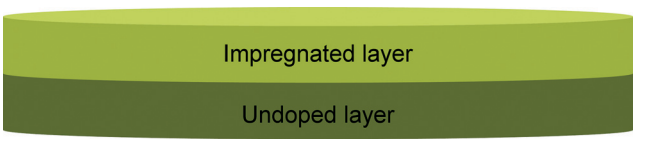


Fig. 2 Principle sketch of two-layer pellet.

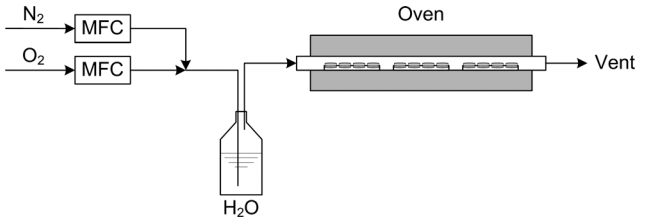


Fig. 3 Schematic drawing of the lab-scale setup for exposure of two-layer pellets.

exposure, a gas mixture of 6 vol% $O_2$ and 3 vol% $H_2O$ in $N_2$ was passed through the reactor at a flow rate of about 1000 NmL $min^{-1}$. The $H_2O$ content was achieved by saturating the $O_2/N_2$ mixture in a water filled bubble flask at room temperature.

### 2.7. Catalyst characterization

The distribution of potassium in exposed plates and pellets was measured at Haldor Topsøe A/S using SEM-EDS (Energy Dispersive X-ray Spectroscopy, Philips XL30 ESEM-FEG) and SEM-WDS (JEOL JXA-8530F HyperProbe) respectively. The samples (small plate bits or halved pellets) were embedded in epoxy and polished with SiC-paper without using water. In order to avoid charging in the microscope, the specimens were coated with a conductive layer of carbon.

## 3. Results and discussion

### 3.1. Characterization of aerosols in bench-scale reactor

To study the potassium poisoning as a function of aerosol size distribution, the position of the injector probe was varied between exposure campaigns. Two fixed positions were used – one close to the burner outlet, where the flue gas temperature was 1050–1100 °C, and one further downstream, where the temperature at the injection point was about 550 °C. Fig. 4 shows the mass based size distribution, measured by the LPI during injection of KCl solution, at the two respective probe positions. Injecting the solution at the burner outlet resulted in a size distribution with a peak at about 0.12 μm and a geometric mass mean diameter of around 0.15 μm. This mean diameter is only half of that observed by Zheng *et al.* during KCl injection in the same bench-scale setup at a similar temperature.[14] This may be related to a significant difference in the concentration of the injected KCl solution between the two experiments (7.4 g $L^{-1}$ *vs.* 37.3 g $L^{-1}$). In the present study, the salt concentration was kept relatively low in order to avoid clogging of the two-fluid nozzle. An aerodynamic (mass mean) diameter of 0.15 μm roughly corresponds to a Stokes diameter of 0.1 μm for a KCl aerosol. Christensen and co-workers[11,12] measured the size distributions of the aerosols in the flue gas from two different straw fired boilers. Through several measurements the authors obtained mass mean Stokes diameters of 0.2–0.6 μm which are 2–6 times larger than we observed in the bench-scale setup at the given probe position. While the particles obtained in the setup were rather small, particles in this size range are indeed present in the flue gas from full-scale biomass fired power plants.[15] Injecting the KCl solution further downstream the burner resulted in a particle size distribution peaking at 2.6 μm and with a geometric mass mean (aerodynamic) diameter of 1.1 μm, corresponding to a Stokes diameter of around 0.8 μm. At the lower flue gas temperature at this injection point, the aerosol particles will form by drying of the droplets created at the two-fluid nozzle rather than nucleation of particles from KCl molecules in the gas phase, resulting in particles which are somewhat larger than those observed by Christensen and co-workers[11,12] in full-scale plants.

When injecting a $K_2SO_4$ solution at the two different positions, no significant difference between the particle size distributions were obtained, as seen in Fig. 5. Both distributions peak at 1.3 μm and the geometric mass mean (aerodynamic)

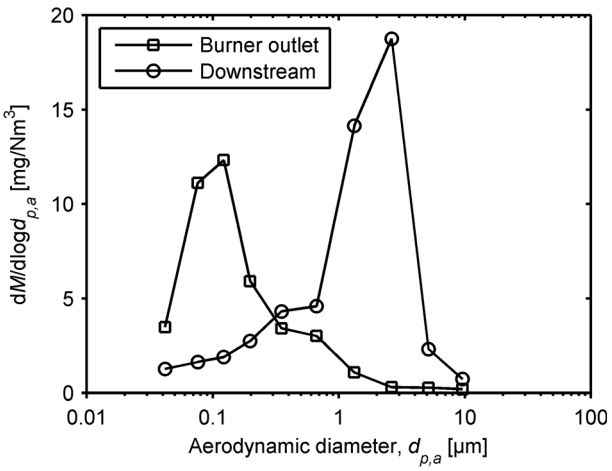


Fig. 4 Mass based size distributions obtained during injection of a 0.1 M KCl solution at 420 mL $h^{-1}$ at the burner outlet (flue gas temperature ≈ 1075 °C) as well as downstream the burner (flue gas temperature ≈ 550 °C).

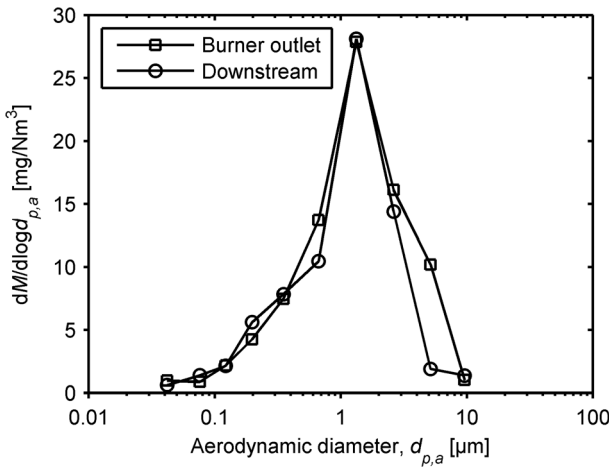


Fig. 5 Mass based size distributions obtained during injection of a 0.05 M $K_2SO_4$ solution at 420 mL $h^{-1}$ at the burner outlet (flue gas temperature ≈ 1075 °C) as well as downstream the burner (flue gas temperature ≈ 550 °C).

diameters are 1.2 μm (burner outlet) and 1.0 μm (downstream) respectively, corresponding to Stokes diameters of approximately 0.7 and 0.6 μm for $K_2SO_4$ aerosols. Due to the low vapor pressure of $K_2SO_4$, the aerosol was thus mostly formed by drying of droplets at both probe positions. The distributions measured for the $K_2SO_4$ aerosols correlate well with the observations by Zheng *et al.*[14]

### 3.2. Ammonia chemisorption on fresh catalysts

The measured $NH_3$ chemisorption capacities of fresh SCR catalysts are listed in Table 1. Each value in the table is an average of at least two successive chemisorption measurements. The repeatability was in all cases excellent. For catalysts which have not been promoted with $WO_3$, the $NH_3$ chemisorption capacity, and thereby the amount of active acid sites, increases with the $V_2O_5$ content, however only slightly when going from 3 to 6 wt% (from 66 to 70 μmol $g^{-1}$). For catalysts promoted with 7 wt% $WO_3$ the $NH_3$ chemisorption capacity does not seem to depend on the $V_2O_5$ content. Both the promoted samples with 1 wt% and the one 6 wt% $V_2O_5$ showed an $NH_3$ chemisorption capacity of 81 μmol $g^{-1}$. This value was in both cases higher than that of the unpromoted counterpart of the respective sample. The $NH_3$ chemisorption capacity of the 3 wt% $V_2O_5$ sample was 66 μmol $g^{-1}$ both with and without $WO_3$ promotion. In general, the results indicate that $WO_3$ promotion increases the total amount of active acid sites and that this amount will be more or less constant, for the given $WO_3$ loading, regardless of the $V_2O_5$ content.

### 3.3. Deactivation of aerosol exposed plates

The absolute activity of fresh, unexposed catalysts, not reported here, was generally higher (by a factor of 1.2–12.6 at 350 °C) for $WO_3$ promoted samples as reported by other researchers.[30–32] Furthermore, the activity increased with the $V_2O_5$ content at temperatures below 400 °C.

Fig. 6 shows the relative activities of 3% $V_2O_5$–7% $WO_3$/$TiO_2$ catalysts exposed to KCl aerosols in four different campaigns, as a function of temperature. In three of the campaigns the two-fluid nozzle was positioned close to the burner outlet in order to ensure evaporation of the injected KCl solutions and the subsequent formation of submicron aerosol particles. In one of the campaigns the solution was injected into a colder flue gas (downstream burner position) in order to create larger particles (>1 μm). As discussed in the Introduction, we speculate larger particles to be less harmful to the SCR catalyst since the deposition rate is lower[14,15] and since the contact area between catalyst surface and potassium rich particles, deposited on the catalyst exterior, will be lower. As seen from the figure, the catalysts exposed in the four campaigns all show significant deactivation. The relative activity of the catalysts exposed at 350 °C for 600 or 300 hours is comparable and very low (<5%). The sample exposed at 150 °C for 300 hours shows higher relative activity compared to the above mentioned samples. This indicates that the mobility of potassium is lower at reduced temperature, since the particle deposition rate is relatively temperature independent. The relative activity of the given sample decreases with increasing temperature which may indicate a shift in the selectivity towards ammonia oxidation. Another explanation could be further deactivation of the sample as the temperature was increased during the activity test. This is, however, unlikely since the activity at 350 °C was measured twice, first when stepwise increasing the temperature from 250 to 400 °C and once more after the 400 °C measurement had been carried out. As seen from Fig. 6, the catalyst activity at 350 °C is unchanged after having been operated at 400 °C. The sample exposed to large aerosol particles at 300 °C for 300 hours is only slightly more active than the catalysts exposed to the aerosol of smaller particles. While the LPI measurements (Fig. 4) showed a clear shift in the particle size distribution towards larger particles when injecting the KCl solution into a colder flue gas, the catalyst may still have been subjected to a significant amount of ultrafine particles due to deposits of KCl on the wall in the high temperature zone. While the major part of these deposits had been removed before the experiment with large

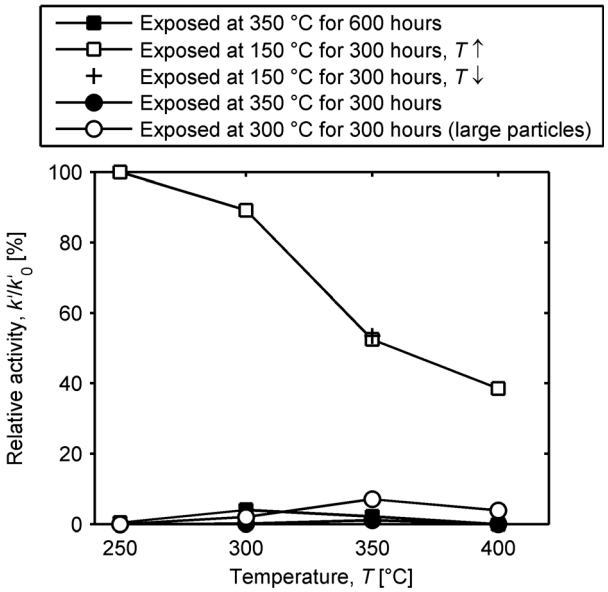


**Fig. 6** Relative catalytic activities of KCl exposed 3% $V_2O_5$–7% $WO_3$/$TiO_2$ catalysts as functions of temperature. Measurement conditions: [NO] = 500 ppmv, [$NH_3$] = 600 ppmv, [$O_2$] = 5 vol%, [$H_2O$] ≈ 1.4 vol%, balance $N_2$. Total flow = 2800 mL $min^{-1}$.

**Table 1** $NH_3$ chemisorption capacities of $V_2O_5$–($WO_3$)/$TiO_2$ catalysts measured at 250 °C

| $V_2O_5$ content [wt%] | $NH_3$ chemisorption capacity [μmol $g^{-1}$] | |
|---|---|---|
| | 0 wt% $WO_3$ | 7 wt% $WO_3$ |
| 1 | 41 | 81 |
| 3 | 66 | 66 |
| 6 | 70 | 81 |

particles was initiated, the presence of a minor residue cannot be excluded. A further investigation on this issue is needed.

Relative activities, measured at 350 °C, of exposed samples of other compositions are given in Table 2. These show similar deactivation trends as the 3% $V_2O_5$–7% $WO_3/TiO_2$ samples. The relative activity of the respective samples exposed at 350 °C for either 600 or 300 hours (entries 1a–3b and 7a–9b in Table 2) are generally low and counter intuitively tends to be lowest for samples exposed for 300 hours. This may, however, be accredited to measurement uncertainties which are enhanced when the activities of the exposed samples are very low.

For the 1% $V_2O_5/TiO_2$ sample exposed at 350 °C for 300 hours (7a), no SCR activity could be measured. The same catalyst exposed for 600 hours (1a) shows a remaining activity of 24% at 350 °C. This may again be due to uncertainties caused by the fact that the initial activity of the given catalyst is fairly low. There may also be variations in the amount of aerosol each plate has been exposed to, depending on its position in the cassette. The general trend in the data is nevertheless clear.

As was the case for the 3% $V_2O_5$–7% $WO_3/TiO_2$ sample exposed to KCl at 150 °C for 300 hours (Fig. 6 and 5b in Table 2), the other samples exposed in this campaign (4a–5a, 6a and 6b in Table 2) also show higher remaining activities compared to those exposed at higher temperatures, again indicating reduced mobility of potassium at 150 °C compared to 350 °C. There does not seem to be a clear influence of the $V_2O_5$ content on the degree of deactivation. However, except for the aforementioned sample 7a, the 1 wt% $V_2O_5$ catalysts without $WO_3$ (1a and 4a) retain a larger fraction of their initial activity compared to $WO_3$ free samples with higher $V_2O_5$ loadings. Furthermore, the relative activity of the unpromoted samples exposed at 350 °C for 600 hours (1–3a) decreases with increasing $V_2O_5$ content. The increased deactivation rate of the samples with high $V_2O_5$ loadings may be caused by an increased abundance of active Brønsted acid sites, as indicated by the $NH_3$ chemisorption data in Table 1, over which potassium may diffuse. A similar trend cannot be observed for $WO_3$ promoted samples, indicating that any effect on the deactivation rate by variations in the $V_2O_5$ loading is masked by the relatively high content of $WO_3$. This too correlates with the observations from the chemisorption measurements. In five out of the six cases where the activity of KCl exposed samples have been measured for catalysts both with and without $WO_3$, and where relative activity at 350 °C is above 10% for at least one of the samples in the 0% $WO_3$/7% $WO_3$ pair (1ab, 2ab, 4ab–6ab and 8ab), the $WO_3$ promoted samples have lost a larger fraction of their initial activity compared to the unpromoted ones. This is *e.g.* the case for the 1% $V_2O_5$–(7% $WO_3$)/$TiO_2$ catalysts exposed at 150 °C for 300 hours where the unpromoted sample (4a) has retained 77% of its initial activity, while the promoted sample (4b) only has retained 29%. This indicates that the increased Brønsted acidity provided by the $WO_3$,[33–36] apart from enhancing the initial activity, facilitates the transport of potassium in the catalysts, in a similar fashion as the Brønsted acid sites from $V_2O_5$, accelerating the poisoning.

The relative activities of 3% $V_2O_5$–7% $WO_3/TiO_2$ catalysts exposed to $K_2SO_4$ aerosols are shown in Fig. 7. As seen from the figure, the sample exposed at 300 °C for 72 hours shows the highest relative activity of the four samples, only deviating from 100% at temperatures above 300 °C. The sample exposed at 150 °C for the same amount of time has lost a slightly larger fraction of its initial activity. The fact that the sample exposed at the highest temperature has deactivated the least contradicts the observations from the KCl exposed catalysts. This might be due to an initial activity drop during the first hours of exposure which may vary from catalyst to catalyst, and which is less dependent on exposure conditions. Furthermore, small variations in the amount of aerosol the

**Table 2** Exposure conditions and relative activities of $V_2O_5$–$(WO_3)/TiO_2$ catalysts

| Entry no. | $V_2O_5$ content [wt%] | Potassium source | Temperature [°C] | Time [h] | Aerosol distribution mode [μm] | Relative activity at 350 °C [%] | |
|---|---|---|---|---|---|---|---|
| | | | | | | a) 0 wt% $WO_3$ | b) 7 wt% $WO_3$ |
| 1 | 1 | KCl | 350 | 600 | 0.12 | 24 | 11 |
| 2 | 3 | KCl | 350 | 600 | 0.12 | 19 | 2 |
| 3 | 6 | KCl | 350 | 600 | 0.12 | 1 | 4 |
| 4 | 1 | KCl | 150 | 300 | 0.12 | 77 | 29 |
| 5 | 3 | KCl | 150 | 300 | 0.12 | 32 | 52 |
| 6 | 6 | KCl | 150 | 300 | 0.12 | 47 | 34 |
| 7 | 1 | KCl | 350 | 300 | 0.12 | 0 | 6 |
| 8 | 3 | KCl | 350 | 300 | 0.12 | 14 | 1 |
| 9 | 6 | KCl | 350 | 300 | 0.12 | 2 | 3 |
| 10 | 3 | KCl | 300 | 300 | 2.6 | n.p.[a] | 7 |
| 11 | 6 | KCl | 300 | 300 | 2.6 | n.p. | 1 |
| 12 | 3 | $K_2SO_4$ | 150 | 72 | 1.3 | n.p. | 84 |
| 13 | 3 | $K_2SO_4$ | 150 | 240 | 1.3 | 77 | 64 |
| 14 | 3 | $K_2SO_4$ | 300 | 72 | 1.3 | n.p. | 95 |
| 15 | 3 | $K_2SO_4$ | 300 | 240 | 1.3 | 37 | 50 |

[a] n.p.: experiment not performed.

 

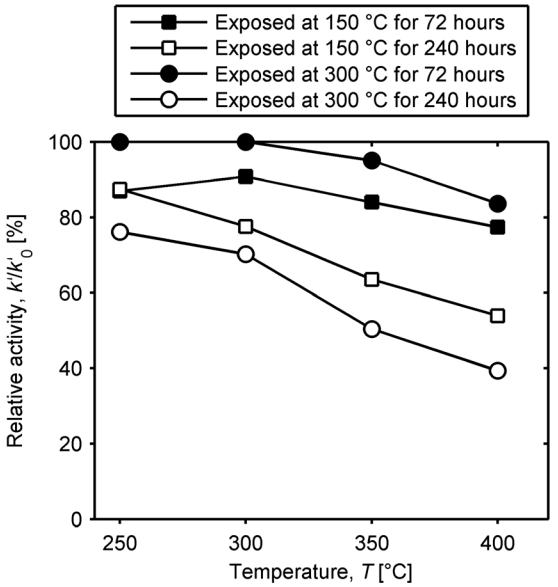


**Fig. 7** Relative catalytic activities of $K_2SO_4$ exposed 3% $V_2O_5$–7% $WO_3$/$TiO_2$ catalysts as functions of temperature. Measurement conditions: [NO] = 500 ppmv, [$NH_3$] = 600 ppmv, [$O_2$] = 5 vol%, [$H_2O$] ≈ 1.4 vol%, balance $N_2$. Total flow = 2800 mL $min^{-1}$.

individual catalyst has been exposed to, *e.g.* due to being positioned differently in the cassette, may have a relatively large effect on the activity in the beginning of an exposure campaign. After 240 hours of exposure, both samples have deactivated further, and the sample exposed at 150 °C shows higher relative activity than that subjected to a $K_2SO_4$ aerosol at 300 °C, as expected. The $K_2SO_4$ exposed catalysts have deactivated significantly less compared to samples exposed to KCl at similar conditions, and the deactivation seem to be less temperature dependent. This indicates that $K_2SO_4$ is less poisonous compared to KCl, as previously reported by Zheng *et al.*[10,14] However, as explained earlier, the particles generated during $K_2SO_4$ injection tended to be larger than those formed under KCl injection. Thus, an effect of particle size on the degree of deactivation cannot be excluded.

Table 2 lists relative activities (measured at 350 °C) of both unpromoted and $WO_3$ promoted 3% $V_2O_5$/$TiO_2$ catalysts exposed to $K_2SO_4$ aerosols (entries 12b–15b). As for the $WO_3$ promoted samples (Fig. 7, 13b and 15b in Table 2) the unpromoted samples exposed for 240 hours show lower activity at the higher exposure temperature of 300 °C compared to exposure at 150 °C, once again indicating that the mobility of potassium is reduced at lower operating temperatures. Reducing the operating temperature of the SCR unit in a power plant would of course mean a lower $NO_x$ conversion per layer of catalyst, which in turn would require additional catalyst layers in order to obtain the desired $NO_x$ reduction. Whether or not a prolonged life-time of the SCR catalyst is worth such a trade-off is outside the scope of this paper. However, low-dust SCR units have been successfully operated at some wood fired boilers at temperatures as low as 160 °C, leading to significantly reduced deactivation rates, indicating promise of such a strategy.[37]

The significant deactivation observed for the catalyst plates, after only a few hundred hours of exposure in the bench-scale setup, is more severe than what is observed in full-scale biomass fired plants.[13,15,38] One explanation could be that the particles produced in the bench-scale setup, in several of the experiments, were smaller than those observed in full-scale plants, as previously discussed. Furthermore, the catalysts exposed in the bench-scale reactor were subjected to the pure potassium salts. In a full-scale plant, the deposited particles may contain other elements such as silicon and calcium.[11,15,38] The presence of compounds containing these elements may, to some extent, delay the potassium poisoning of the catalyst, either by dilution or by binding[39] a fraction of the potassium as inert species.

### 3.4. Potassium profiles in exposed plates

Fig. 8 shows the SEM-EDS measured K/V molar ratios across the wall of three 3% $V_2O_5$–7% $WO_3$/$TiO_2$ catalyst plates exposed to either KCl or $K_2SO_4$ aerosols at various temperatures and exposure times. As seen from the figure, the thickness of the individual plates varied between 900 to about 1400 μm. The plate exposed to KCl at 350 °C for 600 hours has the highest K/V ratio, throughout its thickness, of the three specimens. Very high K/V ratios can be observed near the edges of the samples which drop steeply to a near constant level inside the catalyst. The average K/V ratio calculated at the distance from 100 to 800 μm is 0.60. For a 3% $V_2O_5$–$WO_3$/$TiO_2$ catalyst impregnated with KCl to a K/V ratio of 0.4, Zheng *et al.*[10] reported a remaining activity of about 40% at 250 °C, while a K/V ratio of 0.7 reduced activity to around 10% of its original value. Chen and co-workers[16,40] reported an activity loss of approximately 90% at 300 °C for a 5% $V_2O_5$/$TiO_2$ catalyst impregnated with $KNO_3$ to a K/V ratio of about 0.5, while data from Kamata *et al.*[17] show a decrease in activity of nearly 70% at 360 °C for a 1% $V_2O_5$–8% $WO_3$/$TiO_2$ catalyst containing 0.3 wt% $K_2O$ (from $KNO_3$ impregnation), corresponding to a K/V molar ratio of about 0.6.

Larsson *et al.*[41] only observed small effects on the activity upon exposing 1% $V_2O_5$–$WO_3$/$TiO_2$ monoliths to aerosols of KCl and $K_2SO_4$. Even though the authors measured potassium concentrations above 1 wt% (corresponding to K/V molar ratios above 2.3), at penetration depths of up to 650 μm, inside the catalyst walls, the KCl and $K_2SO_4$ aerosol exposed catalysts respectively retained 86 and 98% of their initial activity at 350 °C. Conversely, Larsson *et al.*[41] observed relative activities of 50 and 56% in similar catalysts, respectively impregnated with KCl and $K_2SO_4$, although lower potassium concentrations of about 0.2 wt% (corresponding to K/V molar ratios of around 0.5) were detected in the catalysts. While the catalysts and/or test conditions in these studies are not entirely comparable to those in the present study, a K/V ratio of 0.60 does not seem to fully explain the complete deactivation observed for the given catalyst, as illustrated in

Fig. 6. The slight discrepancy between the activity and the K/V ratio of the catalyst may have arisen during the preparation of the activity measurement. When a section of the catalyst plate was crushed down, KCl particles deposited on the external surface of that section will be mixed into the catalyst powder possibly allowing for further potassium spreading and deactivation of the catalyst, either during the crushing procedure and/or during the actual activity measurement where the catalyst powder is heated. No further deactivation of the catalysts over time was however observed during the performed activity measurements.

The K/V ratios through the two remaining samples, *i.e.* the one exposed to KCl at 150 °C for 300 hours and the one exposed to $K_2SO_4$ at 300 °C for 240 hours, are low, around or below 0.1. Some large peaks in the K/V ratio can be observed inside the first of the two, however these are artifacts from where the electron beam hits a ceramic fiber, which may contain small amounts of potassium and no vanadium. The low K/V ratios in the two latter samples are in good agreement with their higher remaining activity compared to the first sample although they might not explain the observed deactivation of about 50% at 350 °C. At lower temperatures, however, these specimens retained most of their initial activity as seen from Fig. 6 and 7.

### 3.5. Potassium mobility in two-layer pellets

Fig. 9 shows the potassium profiles in an unexposed two-layer pellet as well as in pellets exposed for 2 and 7 days, measured by SEM-WDS analysis. The impregnated layer in these pellets was made from a 3% $V_2O_5$–$WO_3/TiO_2$ catalyst doped with an aqueous KCl solution to a potassium level of about 1.6 wt%, corresponding to a molar K/V ratio of 1.2 (nominal). In this particular case, the powdered catalyst had not been calcined subsequent to the KCl impregnation. Even for the unexposed pellet, potassium has, surprisingly, partly diffused into the undoped layer, as seen from the figure. The potassium concentration in the pellets exposed for 2 and 7 days are comparable. While the concentration drops through the impregnated layer, it seems to be leveling out at around 0.6 wt% potassium in the undoped layer, corresponding to a K/V ratio of about 0.5. This K/V ratio is comparable to that found in the catalyst plate exposed to KCl aerosols at 350 °C for 600 hours (see Fig. 8), which indicates that there exists a saturation level at which potassium does no longer diffuse into the SCR catalyst. This level would be expected to correspond to the concentration of Brønsted acid sites. Fig. 10 shows the chlorine level in the same three pellets. As seen from the figure, a significant amount of chlorine is present in the impregnated layer of the unexposed pellet, which correlates well with the amount of potassium in the specimen. No chlorine, however, is present in the undoped layer. The two exposed samples, however, are chlorine free all the way through, indicating that chlorine readily leaves the sample (likely as HCl) when exposed to a flow of $N_2$, $O_2$ and $H_2O$ at 350 °C. This is in agreement with the observations by Wu

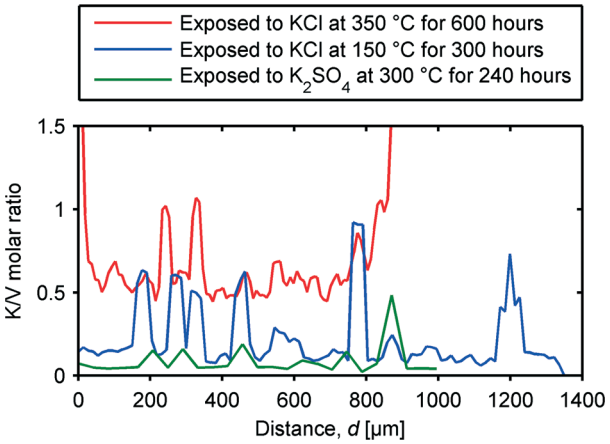


**Fig. 8** K/V molar ratios across the thickness of 3% $V_2O_5$–7% $WO_3/TiO_2$ catalyst plates exposed to aerosols of KCl or $K_2SO_4$.

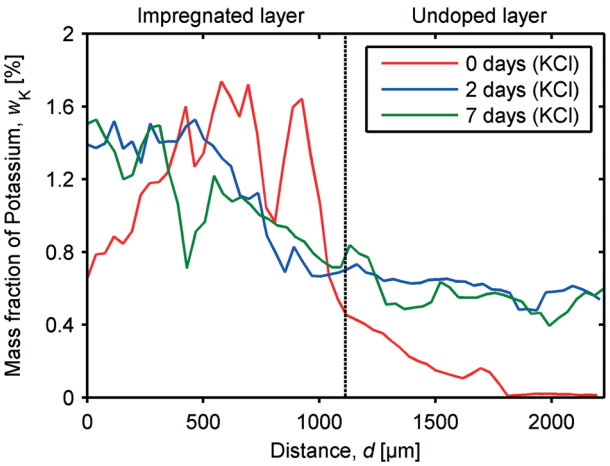


**Fig. 9** Potassium profiles in KCl impregnated (1.6 wt% K, nominal) two-layer pellets of 3% $V_2O_5$–$WO_3/TiO_2$ catalyst, exposed to a flow (1000 NmL $min^{-1}$) of 6 vol% $O_2$ and 3 vol% $H_2O$ in $N_2$ at 350 °C for 0–7 days.

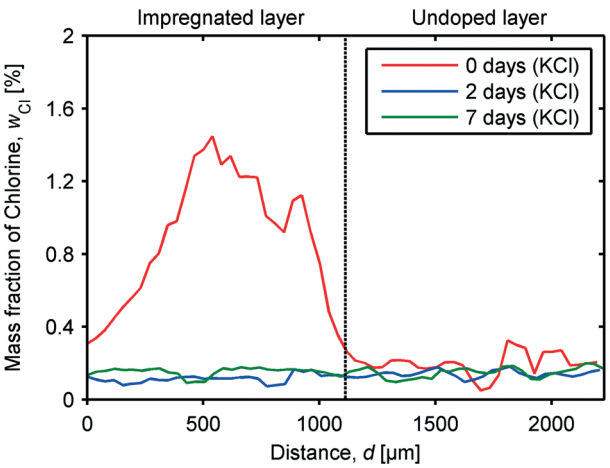


**Fig. 10** Chlorine profiles in KCl impregnated (1.6 wt% K, nominal) two-layer pellets of 3% $V_2O_5$–$WO_3/TiO_2$ catalyst, exposed to a flow (1000 NmL $min^{-1}$) of 6 vol% $O_2$ and 3 vol% $H_2O$ in $N_2$ at 350 °C for 0–7 days.

*et al.*[21] who only found a minute chlorine level in a KCl impregnated SCR catalyst after calcination at 400 °C for 2 hours. This implies that potassium has to coordinate to something else when left behind by its counter ion, most likely being the Brønsted acid sites on the catalyst.[10,14,16–22]

The above observations indicate that the potassium transport in SCR catalysts involves two steps: 1) reaction between salt bound potassium and catalyst surface, and 2) diffusion of potassium over the surface. The latter appears to be fast, judging from the rather flat potassium profiles in the undoped layers of the exposed pellets in Fig. 9. Before heat treatment of a pellet, potassium is present in the impregnated layer as salt particles, in intimate contact with the catalyst material, and possibly also as surface bound potassium. The latter may explain the movement of potassium into the undoped layer before heat treatment. For an aerosol exposed SCR catalyst, only the external surface will be in close contact with ultrafine potassium salt particles, and thus the potassium transport, into the catalyst, will be slower. Fig. 11 shows the potassium profile in a two-layer pellet consisting of a layer of pure KCl (particles size $< 250$ μm) and a layer of 3% $V_2O_5$–7% $WO_3/TiO_2$ catalyst, exposed for 7 days. As seen from the figure, no potassium has moved into the catalyst layer. This implies that the salt particles not only have to be in close contact with the catalyst, in order for potassium to leave the salt in reaction with the surface, the particles also need to be very small – most likely in the submicron range. A similar conclusion was obtained by Zheng *et al.*[14] They exposed catalyst plates with deposits of KCl particles (with a mean diameter of 350 μm) to 200 NmL $min^{-1}$ of air with about 3 vol% $H_2O$ and 1000 ppm $SO_2$ at 350 °C. After exposure for nearly 2400 hours, the catalysts had only lost 13% of their initial activity at 350 °C. The reason for the much slower transport of potassium from the pure KCl layer, into the catalyst, is probably due to a lower contact area between the particles and the catalyst, despite the compression during the pellet formation.

The potassium level in three two-layer pellets of 3% $V_2O_5$–$WO_3/TiO_2$ catalyst with $K_2SO_4$ impregnated layers are shown in Fig. 12. Two of the pellets have impregnated layers initially containing about 0.8 wt% potassium (K/V ≈ 0.6), while the third pellet has a layer doped to a potassium level of approximately 1.6 wt%. One pellet is unexposed while two others have been exposed for 8 hours. For comparison, the potassium profile in a pellet with a KCl impregnated layer (0.8 wt% potassium), also exposed for 8 hours, has been included as well. Similar to the impregnation with KCl, some potassium has moved into the undoped layer prior to exposure. Looking at the exposed pellets with impregnated layers containing 0.8 wt% potassium from either $K_2SO_4$ or KCl, there is a significant difference in the potassium level in the undoped layers. For the pellet with the $K_2SO_4$ impregnated layer the potassium concentration has increased slightly compared to that in the unexposed pellet, and is essentially zero half way through the undoped layer, while the potassium level in the undoped layer of the pellet with the KCl impregnated layer is considerably higher. In the case of the pellet with the impregnated layer doped with 1.6 wt% potassium from $K_2SO_4$, the potassium level in the undoped side, upon exposure for 8 hours, is comparable to that of the KCl impregnated pellet. Hence, potassium from $K_2SO_4$ appears to be half as mobile as that of KCl.

Fig. 13 shows the sulfur level in the two pellets with $K_2SO_4$ impregnated layers. Unlike chlorine, the sulfur stays in the impregnated layer both before and after exposure. These observations may explain the apparent difference in mobility between potassium bound in KCl and $K_2SO_4$. It is speculated that in order for salt bound potassium to diffuse into the undoped layer, it first needs to react with a

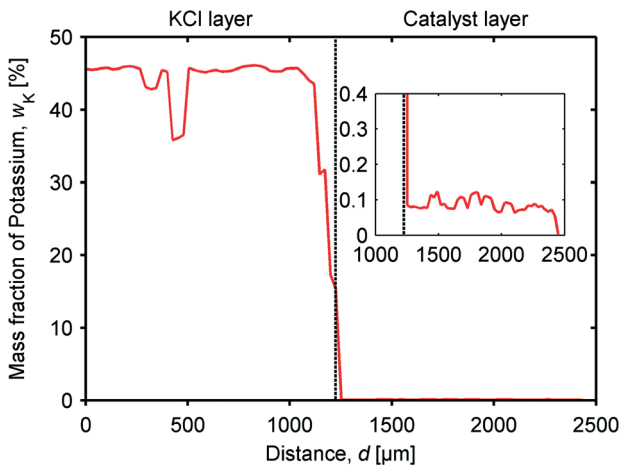


**Fig. 11** Potassium profile in a two-layer pellet containing a layer of pure KCl and a layer of a 3% $V_2O_5$–7% $WO_3/TiO_2$ catalyst, exposed to a flow (1000 NmL $min^{-1}$) of 6 vol% $O_2$ and 3 vol% $H_2O$ in $N_2$ at 350 °C for 7 days.

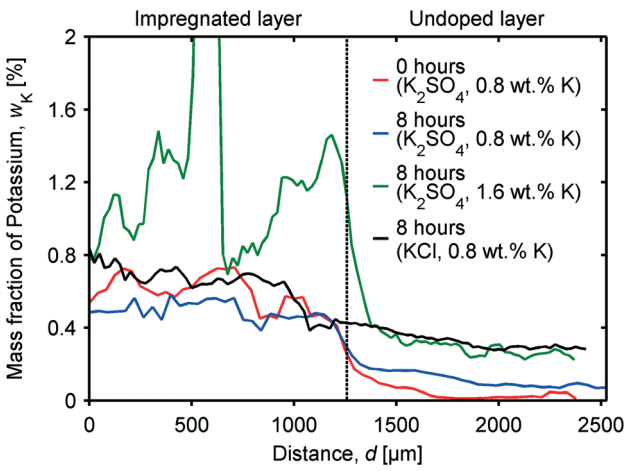


**Fig. 12** Potassium profiles in $K_2SO_4$ or KCl impregnated (0.8–1.6 wt% K, nominal) two-layer pellets of 3% $V_2O_5$–$WO_3/TiO_2$ catalyst, exposed to a flow (1000 NmL $min^{-1}$) of 6 vol% $O_2$ and 3 vol% $H_2O$ in $N_2$ at 350 °C for 0–8 hours.

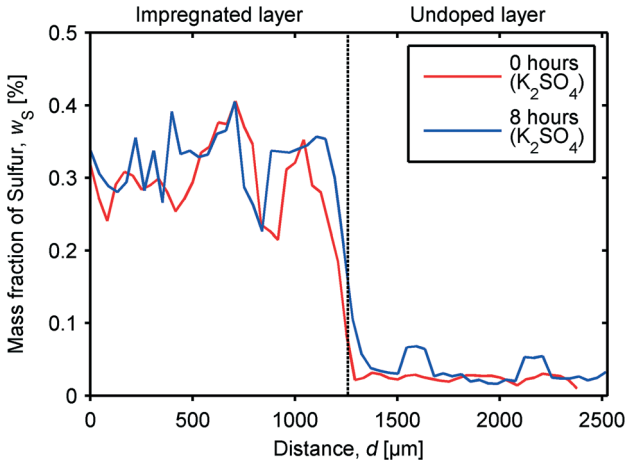


**Fig. 13** Sulfur profiles in $K_2SO_4$ impregnated (0.8 wt% K, nominal) two-layer pellets of 3% $V_2O_5$–$WO_3$/$TiO_2$ catalyst, exposed to a flow (1000 NmL min$^{-1}$) of 6 vol% $O_2$ and 3 vol% $H_2O$ in $N_2$ at 350 °C for 0–8 hours.

Brønsted acid site on the catalyst, *e.g.* through the following reactions:[10]

$$\text{–M–OH} + \text{KCl} \xrightarrow{k_{\text{KCl}}} \text{–M–OK} + \text{HCl} \quad (5)$$

$$\text{–M–OH} + \text{K}_2\text{SO}_4 \overset{k_{\text{K}_2\text{SO}_4}}{\rightleftarrows} \text{–M–OK} + \text{KHSO}_4 \quad (6)$$

$$\text{–M–OH} + \text{KHSO}_4 \overset{k_{\text{KHSO}_4}}{\rightleftarrows} \text{–M–OK} + \text{H}_2\text{SO}_4 \quad (7)$$

Where –M–OH is either a vanadium or tungsten Brønsted acid site. A difference between KCl and $K_2SO_4$, as indicated by the results in Fig. 10 and 13, is that the reaction product of the counter ion for KCl (HCl) is gaseous and thus leaves the sample, in this way pulling the reaction towards the right. The sulfur species are either non-volatile at the reaction conditions or significantly less volatile than HCl, which in principle could allow for the reverse reactions. Furthermore, the lattice energy of KCl is significantly lower than that of $K_2SO_4$ (720 kJ mol$^{-1}$ *versus* 1796 kJ mol$^{-1}$),[42] which indicates that $K_2SO_4$ is more stable. Consequently, potassium bound in KCl can more easily escape its solid matrix compared to that bound in $K_2SO_4$ which may partly explain why potassium in KCl acts as a more efficient poison than $K_2SO_4$. $KHSO_4$, which is the product of reaction 6, melts at around 215 °C and may to some extent convert into $K_2S_2O_7$ at temperatures above 300 °C.[43,44] However, if salt melts were formed during exposure of the $K_2SO_4$ impregnated pellets, the sulfur would likely have diffused into the undoped layer, together with potassium. Using the Kapustinskii equation,[42,45] the lattice energy of $KHSO_4$ can be estimated to about 590 kJ mol$^{-1}$. The difference in lattice energies, combined with the fact that chlorine leaves the sample upon short time exposure while sulfur stays in the impregnated layer, as well as the apparent twofold difference in the mobility of potassium from $K_2SO_4$ and KCl, observed in Fig. 12, suggest that the reaction between $K_2SO_4$ and –M–OH sites (6) is much slower than that involving KCl (5), *i.e.* $k_{\text{KCl}} \gg k_{\text{K}_2\text{SO}_4}$. As the estimated lattice energy of $KHSO_4$ is lower than that of KCl, reaction 7 is likely somewhat faster than reaction 5, $k_{\text{KHSO}_4} > k_{\text{KCl}}$.

In order to study the potassium mobility as a function of catalyst composition, a series of two-layer pellets was produced from $V_2O_5$–$WO_3$/$TiO_2$ catalysts with 0, 1, 3 and 6 wt% $V_2O_5$ and 7 wt% $WO_3$. Furthermore, a two-layer pellet of $WO_3$ free 3% $V_2O_5$/$TiO_2$ catalyst and one of pure fiber reinforced $TiO_2$ carrier were produced. In all cases the impregnated layer was made from the respective catalyst doped with KCl to a potassium level of about 1.6 wt%, corresponding to nominal K/V ratios of 3.7, 1.2 and 0.6 for the three different (nonzero) $V_2O_5$ loadings. Fig. 14 shows the potassium profiles in these pellets after exposure for 7 days. For the three pellets of catalyst containing both $V_2O_5$ and $WO_3$ the potassium concentration has reached comparable levels of 0.4–0.5 wt% in the undoped layer. Hence, there does not seem to be a connection between potassium mobility and $V_2O_5$ loading for catalysts with relatively high $WO_3$ loadings. For the 3% $V_2O_5$/$TiO_2$ sample the potassium diffusion seem to have proceeded at a slower rate reaching a potassium level of about 0.25 wt% far inside the undoped layer. Similar levels are found in the 7% $WO_3$/$TiO_2$ pellet and the pellet made from $TiO_2$ carrier. As indicated by the bench-scale tests, the two-layer pellet data further indicate that $WO_3$ promotion facilitates the potassium transport in the SCR catalyst. Furthermore, the higher potassium mobility in $V_2O_5$–$WO_3$/$TiO_2$ catalysts seems to be due to some interaction between $V_2O_5$ and $WO_3$ which is independent on the $V_2O_5$ content. The latter is also in good agreement with the observations from the activity measurements as well as the $NH_3$ chemisorption study.

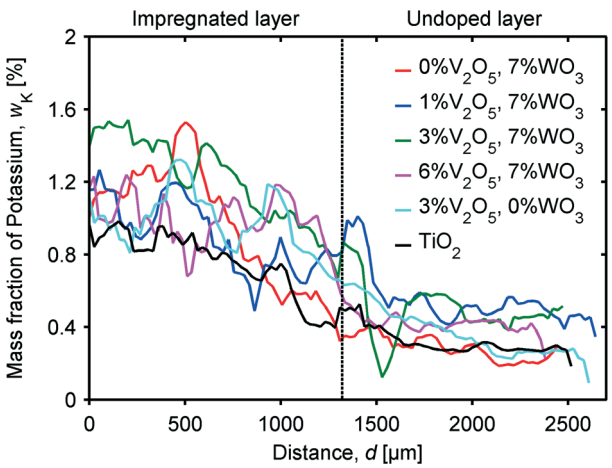


**Fig. 14** Potassium profiles in KCl impregnated (1.6 wt% K, nominal) two-layer pellets of $V_2O_5$–($WO_3$)/$TiO_2$ catalysts, exposed to a flow (1000 NmL min$^{-1}$) of 6 vol% $O_2$ and 3 vol% $H_2O$ in $N_2$ at 350 °C for 7 days.

## 4. Conclusions

Industrial type $V_2O_5$–($WO_3$)/$TiO_2$ SCR catalysts have been exposed to KCl or $K_2SO_4$ aerosols in a bench-scale reactor in order to investigate catalyst deactivation (by potassium poisoning) under biomass firing conditions. All catalysts exposed for 240 hours or longer showed significant deactivation. Samples exposed at 150 °C rather than 300/350 °C, however, showed higher remaining activity indicating decreased potassium mobility with decreasing temperature. The $K_2SO_4$ exposed catalysts had deactivated considerably less than the ones exposed to KCl exposed ones. This could be due to potassium in $K_2SO_4$ being less mobile once deposited on the catalyst, which is supported by the observations from the pellet experiments. In addition, measurements showed that the particle size distribution of the $K_2SO_4$ aerosol obtained in the setup was shifted towards larger particles compared to that of the KCl aerosol, which may lead to a slower deposition rate of particles on the external surface of each catalyst plate, as well as a smaller contact area per mass of aerosol. Hence, an effect of particle size on the catalyst deactivation cannot be excluded.

At large, the relative activity of the exposed catalysts indicates that $WO_3$ promoted samples, which in general have higher $NH_3$ adsorption capacities, have lost a larger fraction of their initial activity compared to unpromoted ones. This implies that increased Brønsted acidity facilitates the potassium transport in the catalyst as well as leads to a higher equilibrium uptake, which supports the proposed theory of diffusion of potassium ions *via* Brønsted acid sites. This is further supported by the results from a study on the potassium mobility in two-layer catalyst pellets of various compositions. It should, however, be noted that the absolute activity of $WO_3$ promoted catalysts in general is significantly higher than for unpromoted samples and so it may not be favorable to use unpromoted catalysts in biomass fired systems.

The potassium mobility in SCR catalysts was studied using a novel experimental method in which pellets composed of two similar layers of catalyst were heat treated. One of the layers was impregnated with KCl or $K_2SO_4$ while the other layer was undoped. These investigations clearly showed that potassium bound in KCl has a much higher mobility in SCR catalysts compared to that in $K_2SO_4$, due to the latter being a more stable salt. While chlorine completely left the catalyst pellet upon treatment at SCR conditions (350 °C, 6 vol% $O_2$ and 3 vol% $H_2O$ in $N_2$), indicating complete conversion of KCl to –M–OK and HCl, sulfur stayed in the sample and was immobile. The results support a view where potassium reacts with and subsequently diffuses over Brønsted acid sites in the catalyst, and that the reaction rate of salt bound potassium (KCl of $K_2SO_4$) is related to how easy potassium is able to leave its counter ion. All together, the results indicate that a lower operating temperature and high conversion of KCl to $K_2SO_4$ will enhance the life-time of an SCR catalyst.

## Acknowledgements

Innovation Fond Denmark is gratefully acknowledged for funding this work which is a part of the GREEN Research Center (DSF-10-093956).

## References

1 H. Bosch and F. Janssen, *Catal. Today*, 1988, **2**(4), 369–532.
2 P. Forzatti, *Appl. Catal., A*, 2001, **222**, 221–236.
3 G. Busca, L. Lietti, G. Ramis and F. Berti, *Appl. Catal., B*, 1998, **18**, 1–36.
4 N.-Y. Topsøe, *Science*, 1994, **265**(5176), 1217–1219.
5 N.-Y. Topsøe, J. A. Dumesic and H. Topsøe, *J. Catal.*, 1995, **151**, 241–252.
6 J. A. Dumesic, N.-Y. Topsøe, H. Topsøe, Y. Chen and T. Slabiak, *J. Catal.*, 1996, **163**, 409–417.
7 A. S. Negreira and J. Wilcox, *J. Phys. Chem. C*, 2013, **117**(46), 24397–24406.
8 A. S. Negreira and J. Wilcox, *Energy Fuels*, 2015, **29**(1), 369–376.
9 B. Sander, *Biomass Bioenergy*, 1997, **12**(3), 177–183.
10 Y. Zheng, A. D. Jensen and J. E. Johnsson, *Ind. Eng. Chem. Res.*, 2004, **43**, 941–947.
11 K. A. Christensen and H. Livbjerg, *Aerosol Sci. Technol.*, 1996, **25**, 185–199.
12 K. A. Christensen, M. Stenholm and H. Livbjerg, *J. Aerosol Sci.*, 1998, **29**(4), 421–444.
13 Y. Zheng, A. D. Jensen and J. E. Johnsson, *Appl. Catal., B*, 2005, **60**, 253–264.
14 Y. Zheng, A. D. Jensen, J. E. Johnsson and J. R. Thøgersen, *Appl. Catal., B*, 2008, **83**, 186–194.
15 Å. Kling, C. Andersson, Å. Myringer, D. Eskilsson and S. G. Järås, *Appl. Catal., B*, 2007, **69**, 240–251.
16 J. P. Chen and R. T. Yang, *J. Catal.*, 1990, **125**, 411–420.
17 H. Kamata, K. Takahashi and C. U. I. Odenbrand, *J. Mol. Catal. A: Chem.*, 1999, **139**, 189–198.
18 D. Nicosia, M. Elsener, O. Kröcher and P. Jansohn, *Top. Catal.*, 2007, **42–43**, 333–336.
19 M. Klimczak, P. Kern, T. Heinzelmann, M. Lucas and P. Claus, *Appl. Catal., B*, 2010, **95**, 39–47.
20 L. Chen, J. Li and M. Ge, *Chem. Eng. J.*, 2011, **170**, 531–537.
21 X. Wu, W. Yu, Z. Si and D. Weng, *Front. Environ. Sci. Eng.*, 2013, 7(3), 420–427.
22 Y. Peng, J. Li, W. Si, J. Luo, Y. Wang, J. Fu, X. Li, J. Crittenden and J. Hao, *Appl. Catal., B*, 2015, **168–169**, 195–202.
23 H. Si-Ahmed, M. Calatayud, C. Minot, E. Lozano Diz, A. E. Lewandowska and M. A. Bañares, *Catal. Today*, 2007, **126**, 96–102.
24 D. Nicosia, I. Czekaj and O. Kröcher, *Appl. Catal., B*, 2008, **77**, 228–236.
25 F. Tang, B. Xu, H. Shi, J. Qiu and Y. Fan, *Appl. Catal., B*, 2010, **94**, 71–76.
26 J. R. Jensen, T. Slabiak and N. White, *Arsenic resistant SCR catalysts*, Haldor Topsøe A/S, Kgs. Lyngby, DK, [Technical

report from the internet], 2009 [Cited November 3, 2015] Available from: http://www.topsoe.com/sites/default/files/arsenic_resistant_scr_catalyst_march_09.ashx__0.pdf.
27 G. Ramis, G. Busca, F. Bregani and P. Forzatti, *Appl. Catal.*, 1990, **64**, 259–278.
28 E. Tronconi, P. Forzatti, J. P. Gomez Martin and S. Malloggi, *Chem. Eng. Sci.*, 1992, **47**(9–11), 2401–2406.
29 M. Koebel and M. Elsener, *Chem. Eng. Sci.*, 1998, **53**(4), 657–669.
30 L. J. Alemany, L. Lietti, N. Ferlazzo, P. Forzatti, G. Busca, E. Giamello and F. Bregani, *J. Catal.*, 1995, **155**, 117–130.
31 L. Lietti, P. Forzatti and F. Bregani, *Ind. Eng. Chem. Res.*, 1996, **35**, 3884–3892.
32 P. G. W. A. Kompio, A. Brückner, F. Hipler, G. Auer, E. Löffler and W. Grünert, *J. Catal.*, 2012, **286**, 237–247.
33 G. Ramis, G. Busca, C. Cristiani, L. Lietti, P. Forzatti and F. Bregani, *Langmuir*, 1992, **8**, 1744–1749.
34 J. P. Chen and R. T. Yang, *Appl. Catal., A*, 1992, **80**, 135–148.
35 L. J. Alemany, F. Berti, G. Busca, G. Ramis, D. Robba, G. P. Toledo and M. Trombetta, *Appl. Catal., B*, 1996, **10**, 299–311.
36 M. D. Amiridis, R. V. Duevel and I. E. Wachs, *Appl. Catal., B*, 1999, **20**, 111–122.
37 H. Jensen-Holm, F. Castellino and T. Nathan White, *SCR DeNOx catalyst considerations when using biomass in power generation*, Haldor Topsøe A/S, Kgs. Lyngby, DK, [Technical report from the internet], 2012 [Cited November 3, 2015] Available from: http://www.topsoe.com/sites/default/files/scr_denox_catalyst_considerations_when_using_biomass_in_power_generation_2012.ashx__0.pdf.
38 R. Khodayari, C. Andersson, C. U. I. Odenbrand and L. H. Andersson, in *Proceedings of the 5th European Conference on Industrial Furnace and Boilers*, Espinho-Porto, Portugal, 2000; *Deactivation and Regeneration of SCR Catalysts used in Bio Fuel Power Plants*, ed. A. Reis, J. Ward, W. Leuckel and R. Collin, INFUB, Rio Tinto, 2000, vol. II, pp. 543–554.
39 L. Wang, J. E. Hustad, Ø. Skreiberg, G. Skjevrak and M. Grønli, *Energy Procedia*, 2012, **20**, 20–29.
40 J. P. Chen, M. A. Buzanowski, R. T. Yang and J. E. Cichanowicz, *J. Air Waste Manage. Assoc.*, 1990, **40**, 1403–1409.
41 A.-C. Larsson, J. Einvall, A. Andersson and M. Sanati, *Energy Fuels*, 2006, **20**(4), 1398–1405.
42 "*Lattice Energies*" *in CRC Handbook of Chemistry and Physics, 96th Edition (Internet Version 2016)*, ed. W. M. Haynes, CRC Press/Taylor and Francis, Boca Raton, FL, 2015.
43 K. M. Eriksen, R. Fehrmann, G. Hatem, M. Gaune-Escard, O. B. Lapina and V. M. Mastikhin, *J. Phys. Chem.*, 1996, **100**(25), 10771–10778.
44 C. B. Knudsen, A. G. Kalampounias, R. Fehrmann and S. Boghosian, *J. Phys. Chem. B*, 2008, **112**(38), 11996–12000.
45 A. F. Kapustinskii, *Q. Rev., Chem. Soc.*, 1956, **10**, 283–294.

 